

# Three D.O.F in a Single Spherical Joint Realized by Omni-Wheels for Industrial Robots

Mustafa W. Abdullah A., Hubert Roth B., Jürgen Wahrburg C., and Kiran Pamanji D.

Institute of Automatic Control Engineering, University of Siegen, Siegen, Germany

Email: abdullah@zess.uni-siegen.de

Michael Weyrich E.

Institute of Automation and Software Engineering, University of Stuttgart, Stuttgart, Germany

**Abstract**—Development on the design concept using Omni-Wheels to provide three degree-of-freedom (d.o.f) in a single spherical joint is presented in this paper. The purpose of this design is to provide the industrial robots that have limited movement flexibility with additional d.o.f in order to carry tasks that require complicated trajectories. In addition, this compact single joint will be installed as an end-effector, therefore there is no need to modify the structure of the industrial robot or to install additional links. Beside the theory and design concept, a model and prototype are created to study the feasibility of such an approach.

**Index Terms**—degree-of-freedom, industrial robot, spherical joint

## I. INTRODUCTION

New processes and applications are introduced in industry yearly, which lead to increase in the demand for industrial robots too. According to the annual report of the International Federation of Robotics there were more than 1.5 millions industrial robots in service by the end of 2013 [1]. However, despite of this big number of deployed industrial robots in different applications in many sectors, the density of robots is around 58 to 10,000 employees in the overall industry's sectors. That means; many applications are still carried by human operators and automated processes that are more efficient in time and quality are not achieved [2]. One of the reasons of this low usage of industrial robots compared to human operators is because of the complexity of the given tasks, such as the assembling of electronic connectors in automotive sector which is not a commercially solved problem. Another reason, that can be found especially in the small and medium size enterprises, is the variation in configuration of given tasks due to either products change or to the enhancement in processes of the production lines [3]. On the other hand, most of the exiting industrial robots were designed to carry specific tasks or for specific applications, such as material handling. Based on the requirements defined by targeted tasks the robot design changes in; shape, degree-of-freedom (d.o.f), and

number of links. Therefore, usually these robots need extra structure configuration or most likely to be replaced with more advances or different types in order to successfully carry the new tasks they were not designed for.

With all the mentioned challenges, the industrial robots are not being considered widely in many sectors and enterprises. Therefore, in order to deal with different applications and trajectories in the same efficiencies as the human operators, the industrial robots should have the ability to perform and ensure the same movement flexibility as the human arm does. In regarding to today robots design and configuration, this mean the industrial robot should have at least six joints to provide the seven d.o.f human arm has. The cornerstone to meet these requirements is, therefore, to provide new types of joints or links structure. In addition to that, these new joints should combine a simplified motion control plus to a compact design comparing to the traditional six joints that is being used in today's industrial robots.

## II. STATE-OF-ART

The research on a solution for a compact and multi d.o.f single joint has started in the mid 1950s by Williams *et al.* by designing a spherical induction motor [4]. In this research, they focused on principles of induction motors and how to control it. On the other hands, Hollis *et al.* proposed a novel six d.o.f magnetically levitated wrist with programmable compliance [5]. The purpose of this wrist was to carry tasks that required high precision and fine compliant motions. With the same targeted problem of improving industrial robot system, Vachtsevanos *et al* build manipulator consists of spherical motor and gripper [6]. Another design of spherical stepper motor in which the stator coils can be energized individually was developed by Lee *et al.* [7]. Taking into account the complexity of stator and rotor in spherical motor, Wang *et al.* proposed new design that has a spherical permanent magnet rotor and three phase stator winding in order to provide two d.o.f [8]. With the aim of designing a motor with high torque and no spatial limitations in motion, Kahlen *et al.* developed spherical motor consist of rotor sphere and carried by 96 poles that controlled individually [9], [10]. By only unitizing three pairs of

Manuscript received May 1, 2015; revised October 21, 2015.

stator coils, Lim *et al.* were able to achieve a three d.o.f in their spherical rotor [11]. Despite of all these effort that spent over the last sixty years on developing a spherical joint or on structures that give same movements flexibility as in spherical joint, there is still no industrial robots use these types of joints in today's markets. This is mainly because of the complicated proposed structures and also control algorithms. Therefore, the need for a compact, multi d.o.f single joint is still present.

### III. PROPOSED APPROACH

The concept of the proposed approach had been introduced previously in [12]. In this paper, the complete kinematic equations, required torque analysis, and the final prototype are explained in details.

#### A. Design Concept

To provide three d.o.f in one single spherical joint as seen in Fig. 1, the proposed concept will differ from the reviewed designs that use coils and stators in electrical motors. Instead, it uses three Omni-Wheels (OWs), which are type of wheels that have small rollers around the circumference, to provide rotation perpendicular to the rolling direction, mounted on a sphere.

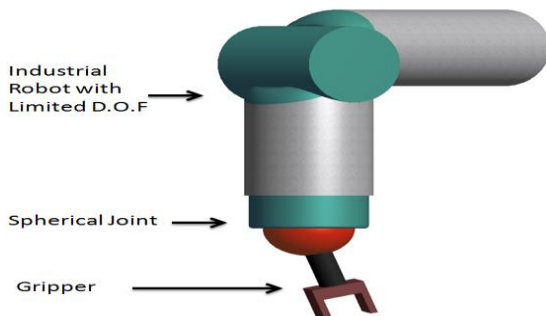


Figure 1. Spherical joint for industrial robot with limited D.O.F.

With calculated locations and alignments of the Omni-wheels on the sphere, it is possible to move the gripper to any desired direction by combined rotations of the sphere on roll, pitch, and yaw. Realization of this rotation of the sphere is based on Omni-wheels' speed and direction. The Omni-wheels are mounted on stepper motors and then they can be controlled based on inverse kinematics which defined the rotation angles to move the gripper to the targeted position.

### IV. KINEMATICS ANALYSIS

There are two main parts in the kinematics of proposed design for the spherical joint; the relationship between the angles of the OWs and the gripper Tool Center Point (TCP) which is defined as the kinematic equation and the second part is the required torques provided by the motors to carry the targeted payload.

#### A. Forward Kinematics

The relationship between the three Omni-Wheels rotation angles ( $\alpha$ ) and TCP position ( $P$ ) as shown in Fig. 3 can be defined as the forward kinematic equation such that:

$$\begin{bmatrix} P_x \\ P_y \\ P_z \end{bmatrix} = f(\alpha_1, \alpha_2, \alpha_3) \quad (1)$$

This equation can be driven from the approach Holland *et al.* used in their Atlas Motion Platforms [13] and the related research reported in [14] and [15]. Following their approach, firstly, the relation between the angular velocities of the Omni-Wheels ( $\omega$ ) and sphere angular velocity ( $\Omega$ ) is found. This is done by finding the linear velocities at the contact points represented first by the OWs local frame:

$$v_k = \omega_k \times r_k \quad (2)$$

where ( $v$ ) is the linear velocity vector, ( $r$ ) is radius vector of the OWs, and  $k = \{1, 2, 3\}$ . From Fig. 2 it can be seen that the OW radius is located on the z-axis of the local frame, hence:

$$r_k = [0 \ 0 \ r_k]^T \quad (3)$$

On the other hand, the rotation of the OW is on x-axis, so the angular velocity can be written as:

$$\omega_k = [0 \ 0 \ \omega_k]^T \quad (4)$$

Knowing that the radiiuses of all OWs are the same, then (2) can be rewritten as:

$$v_1 = \begin{bmatrix} 0 \\ -\omega_1 r_z \\ 0 \end{bmatrix}, v_2 = \begin{bmatrix} -\omega_2 r_z \sin(\beta_2) \\ -\omega_2 r_z \cos(\beta_2) \\ 0 \end{bmatrix}, v_3 = \begin{bmatrix} -\omega_3 r_z \sin(\beta_3) \\ -\omega_3 r_z \cos(\beta_3) \\ 0 \end{bmatrix} \quad (5)$$

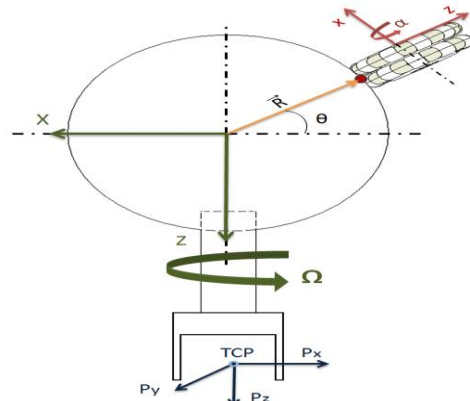


Figure 2. Angular velocities, contact point, and rotation frames.

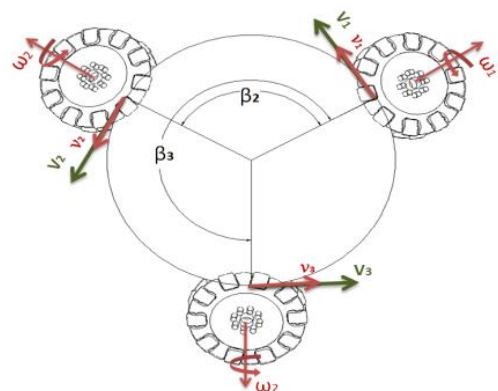


Figure 3. Linear velocities on contact points.

This linear velocity is represented in the local frame of OWs. To rewrite it in the sphere frame a transformation

matrix is needed. By knowing the exact angle between each OW, the transformation matrix can be written as following:

$$T_k = \begin{bmatrix} \cos(\beta_k) & \sin(\beta_k) & 0 \\ -\sin(\beta_k) & \cos(\beta_k) & 0 \\ 0 & 0 & 1 \end{bmatrix} \quad (6)$$

where  $\beta_1 = 0^\circ$ ,  $\beta_2 = 120^\circ$ ,  $\beta_3 = 240^\circ$ .

Therefore, the linear tangential velocity at each contact point can be driven from:

$$V_K = T_K v_K \quad (7)$$

Substitution (5) and (6) into (7), the linear tangential velocity generated by each OW and represented in local frame of the sphere are:

$$V_1 = \begin{bmatrix} 0 \\ -\omega_1 r_z \\ 0 \end{bmatrix}, V_2 = \begin{bmatrix} -\omega_2 r_z \sin(\beta_2) \\ -\omega_2 r_z \cos(\beta_2) \\ 0 \end{bmatrix}, V_3 = \begin{bmatrix} -\omega_3 r_z \sin(\beta_3) \\ -\omega_3 r_z \cos(\beta_3) \\ 0 \end{bmatrix} \quad (8)$$

Similar to the steps followed in finding the angular velocity for OW, the angular velocity of the sphere ( $\Omega$ ) is found from the linear velocity presented in (7), in the local frame of sphere, by cross multiplying with the radial vector ( $R_k$ ) for the contact points as shown in Fig. 3. Thus the inverse cross product to find the angular velocity of the sphere is:

$$\Omega_K = \frac{R_K \times V_K}{\|R\|^2} \quad (9)$$

From Fig. 2 the radial vector ( $R_k$ ) for the contact point is known based on ( $\theta$ ) and ( $\beta$ ) angles that determine the alignment and location of each OW on the sphere respectively. Determining the required angles and the resulted radial vector ( $R_{1x}$ ) and ( $R_{1z}$ ) will be described in the next section. For the general scenario the three radial vectors can be defined as:

$$R_1 = \begin{bmatrix} R_{1x} \\ 0 \\ R_{1z} \end{bmatrix}; R_2 = \begin{bmatrix} \cos(\beta_2) R_{1x} \\ -\sin(\beta_2) R_{1x} \\ R_{1z} \end{bmatrix}; R_3 = \begin{bmatrix} \cos(\beta_3) R_{1x} \\ -\sin(\beta_3) R_{1x} \\ R_{1z} \end{bmatrix} \quad (10)$$

Inserting this result with linear velocity found in (8) into (9), the angular velocity of the sphere as a function of the OW angular velocity is obtained:

$$\begin{bmatrix} \Omega_1 \\ \Omega_2 \\ \Omega_3 \end{bmatrix} = \frac{r_z}{\|R\|^2} \begin{bmatrix} R_{1z} & R_{1z} \cos(\beta_2) & R_{1z} \cos(\beta_3) \\ 0 & -R_{1z} \sin(\beta_2) & -R_{1z} \sin(\beta_3) \\ 0 & 0 & 1 \end{bmatrix} \begin{bmatrix} \omega_1 \\ \omega_2 \\ \omega_3 \end{bmatrix} \quad (11)$$

To find the kinematic equation as function of OWs angle and TCP position vectors, (11) should be integrated first, keeping in mind that the transformation matrix, which will be referred as ( $T_{OW/S}$ ) is a constant. Therefore, integration with respect to time will lead to:

$$\begin{bmatrix} \theta_1 \\ \theta_2 \\ \theta_3 \end{bmatrix} = T_{OW/S} \begin{bmatrix} \alpha_1 \\ \alpha_2 \\ \alpha_3 \end{bmatrix} \quad (12)$$

Next step is to find the transformation matrix from the sphere to the TCP frame as also shown in Fig. 2. To do so, firstly a rotation on Z-axis by 180 is measured. Then, a prismatic displacement is made also on the Z-axis from the center of the sphere to the TCP. The transformation matrix is then:

$$T_{S/TCP} = \begin{bmatrix} \cos(\pi) & \sin(\pi) & 0 \\ -\sin(\pi) & \cos(\pi) & 0 \\ 0 & 0 & d_{TCP} \end{bmatrix} \quad (13)$$

where ( $d_{TCP}$ ) is the displacement between the sphere center and the TCP on z-axis. Using the transformation matrices in (12) and (13), the final kinematic equation as function of OWs' angles as was defined in (1) can be rewritten as:

$$\begin{bmatrix} P_x \\ P_y \\ P_z \end{bmatrix} = T_{OW/S} T_{S/TCP} \begin{bmatrix} \alpha_1 \\ \alpha_2 \\ \alpha_3 \end{bmatrix} \quad (14)$$

### B. Required Torques & Payload

To determine the required torques the OWs should provide, the targeted payload should be assumed first. In the design presented in this research, the payload, i.e. the maximum weight the gripper can carry, is assumed to not be more than to 1.0 kg. Moreover, the gripper and its shaft weights, the sphere moment of inertia should also be considered to determine the required torques from the OWs motors. From the kinematic equation of the system, linear system, it can be seen that the sphere can be rotated by a single OW. Therefore, in driving the required torque equation it is assumed that the total external torques should be equal or less than the torque a single motor will generate. Firstly, the moment of inertia ( $I$ ) of the sphere is calculated as:

$$I_{sphere} = \frac{2}{5} MR^2 \quad (15)$$

where ( $M$ ) and ( $R$ ) are the weight and the radius of the sphere respectively. The locations of the gripper center load and the external load are shown in Fig. 4. Therefore, the torque required from each OW can be driven by the summation of the forces generated by the gripper and payload weights plus the torque required to rotate the solid sphere. The equation of required torque by the OW can be then written as:

$$\tau_{ow} = F_{ow} \times r = I_{sphere} \times \Omega + F_{grip} \times d_{grip} + F_{TCP} \times d_{TCP} \quad (16)$$

Here  $\tau_{ow}$  is torque required by the OW to provide.  $F_{ow}$  is the generated force by OW on contact point.  $r$  is the radius of the sphere.  $\Omega$  is the angular velocity of the sphere.  $F_{grip}$  is the generated force by gripper and shaft weights.  $d_{grip}$  represent the distance between gripper and shaft center of mass and the rotation center.  $F_{TCP}$  is the external force, i.e. payload, applied on TCP. And finally  $d_{TCP}$  is the distance between TCP center and rotation center:

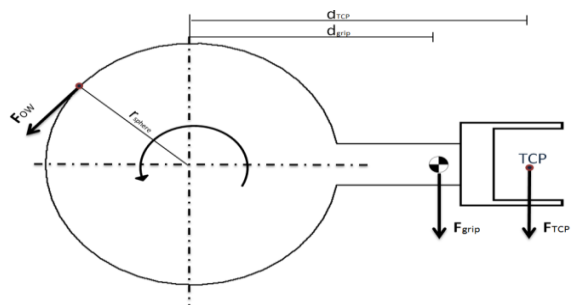


Figure 4. Generated force by Omni-Wheels to equalize the external forces.

## V. PROTOTYPE MODELING & ASSEMBLING

### A. Modifications

There are couples of modifications had been carried out on the proposed prototype in [12]. Firstly, the OWs were replaced with double rollers ones, to increase the contacts point possibilities with the sphere and to reduce the slipping that occurred in the previous design. The rollers on the new OW are made of rubber; therefore, there was no need to coat them with rubber paint again, and only the sphere was coated with a rubber paint to increase the friction. Since one of the OW can rotate the sphere individually as stated previously, the other two should in this case be in free state, i.e. give no resistance to the movement of the sphere. With gearbox motors that were used firstly to provide high torque, this was not possible. Therefore, in the modified prototype, stepper motors with 1.1 [Nm] output torque are used. The structure of prototype was also changed. As a final prototype, there was no need to the adjustable motors holders, since the location of the OWs on the sphere is determine as will be explain later. Lastly, the springs that pulled the motors and OWs toward the sphere where removed and a sufficient contact forces were provided by the Ball Rollers that carries the sphere. The new model design of the complete prototype is shown in Fig. 5.

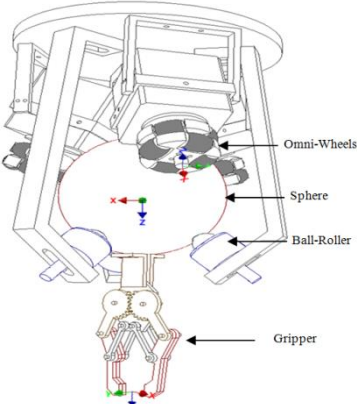


Figure 5. Complete model of the Spherical-Joint.

### B. Omni-Wheels Alignment and Assembling

The alignment, contact location, and number of different types of wheels to rotate the sphere had been deeply instigated by many researchers especially for the Ballbot robots. Lauwers *et al.* [16] used four wheels located on the sphere center axis, however, this alignment make it hard to provide yaw control [17]. Wu *et al.* [18] implemented four OWs firstly, but due to low efficiency of driving forces, they were replaced with chain or rollers mounted orthogonally on the quarter of sphere. This approach also cannot drive a well yaw control with such alignment. To provide, easy and complete control of the sphere rotation, Kumagai and Ochiai [19] proposed a symmetric location of three OWs with 120 degree interval on the sphere. While the alignment in this approach was fixed to 40 degree as is shown in Fig. 8. Different possible configurations of mounting the OWs (i.e. orthogonal, collinear, and symmetric) were studied

by Weiss *et al.* [20]. In the design proposed in this paper, the configuration used by Kumagi and Weiss was selected since it provides non-singular matrix if the alignment angle ( $\theta$ ) was not equal to 0 or  $\pm 90$ . The radius vector for the contact point of the first OW (R1) is located on the z-x plane, and the other two contact points have symmetric location on the planes. The radiiuses components used in (10) and (11) can be driven then from the following:

$$\begin{aligned}\vec{R}_1 &= [R_{1x} \quad R_{1y} \quad R_{1z}]^T = R [\cos(\theta) \quad 0 \quad -\sin(\theta)]^T; \\ \vec{R}_2 &= [R_{2x} \quad R_{2y} \quad R_{2z}]^T = R \left[ -\frac{1}{2}\sin(\theta) \quad \frac{\sqrt{3}}{2}\cos(\theta) \quad -\sin(\theta) \right]^T; \\ \vec{R}_3 &= [R_{3x} \quad R_{3y} \quad R_{3z}]^T = \\ &R \left[ -\frac{1}{2}\sin(\theta) \quad -\frac{\sqrt{3}}{2}\cos(\theta) \quad -\sin(\theta) \right]^T\end{aligned}\quad (17)$$

Using the transformation matrix from (6), and knowing that  $\beta_2=120^\circ$ ,  $\beta_3=240^\circ$ , then (R2) and (R3) vectors can be presented by transferring (R1) to both vectors location individually. The resultant is the transformation matrix presented in (11). Examining the different possibilities in selecting the alignment angle ( $\theta$ ), it can be noticed that, if value is equal to  $0^\circ$ , then the OW will located on the x-axis, i.e. on the x-y plane. Thus, it will be easy to rotate the sphere on z-axis; however, it will not be feasible to be rotated on neither x-axis nor y-axis. On the other hand, if angle is equal to  $90^\circ$ , then the OW will be located on the z-axis, in this case the rotation of the sphere will be easily carried on x-axis, but with same limitation faced in the case of  $0^\circ$ , it not possible to be rotated on z-axis. Furthermore, the determinant of the position matrix that driven from (17) will be equal to zero in the case of ( $\theta=0^\circ$  or  $\pm 90^\circ$ ). Therefore, the alignment angle is selected in the range of ( $0$ – $90^\circ$ ). The alignment angle used in this prototype in this paper stayed the same as in the previous one where  $\theta=40^\circ$ . This is the same alignment angle was reported in [18] and [19].

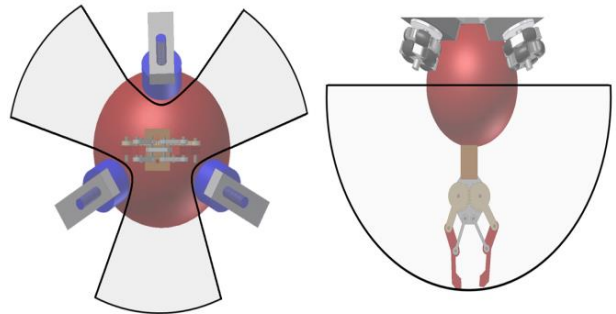


Figure 6. Gripper reachable workspace based on the structural limitations.

### C. Gripper Workspace

In theory, since the sphere can be rotated at any angle on the x, y, and z axes. This mean, based on its length, the gripper can reached any position in a spherical workspace where the radius of this workspace is the distance between the center of the rotating sphere and the TCP of the gripper. However, in the real implementation there are two structural limitations. First one is due OWs and motors attached to the sphere, and the second is from lower part of the sphere due to the carrying ball rollers. In Fig. 6 the possible workspace for the proposed design is

shown. This workspace assumed that the sphere joint is mounted on a fixed ground, and not a robot. Therefore, the lower limitation in the workspace can be eliminated if this prototype spherical joint is attached to an industrial robot that can provide a rotation on the z-axis of the sphere in one or accompanied joints.

## VI. IMPLEMENTATION AND FUTURE WORK

The final design and assembly is shown in Fig. 7. Each stepper motor is controlled individually to satisfy the kinematic equation presented previously. For this purpose, an Arduino AT Mega 2560 microcontroller is used to control; rotation direction, speed, and steps count for each motor. Since the motors have a step of 1.8 degree, a Toshiba 6560 micro-step board is also used. This board can divide the steps up to 1/16 which will lead to provide a fine movement for the OWs on the sphere.

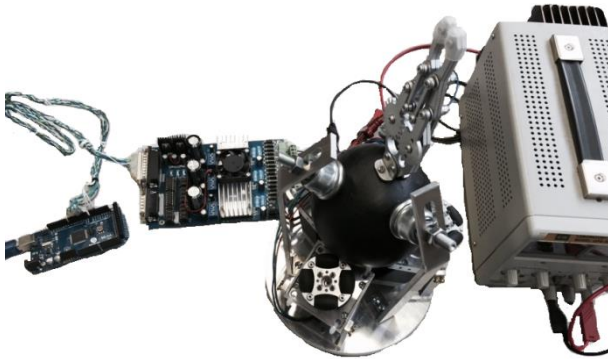


Figure 7. Final prototype assembly with the controller boards.

The controller type is an open loop system. This mean, there is no feedback to ensure that the gripper has reached the desired position that specified in the kinematic equation by the OWs rotation angle. For the future work it is intend to have a close loop control system in which the feedback will come from an accelerometer attached at the gripper. With such a system, the joint can overcome the slipping problem that occurs when high torque is generated. In conclusion, such a design, with the right parameters and high friction between the OWs and sphere can provide the industrial robots that have limited d.o.f. with additional ones, in a single compact end-effector like solution.

## REFERENCES

- [1] Executive Summery World Robotics 2013, International Federation of Robotics–IFR, 2014.
- [2] M. Hägele and J. N. Pires, "Industrial robotics," *Springer Handbook of Robotics*, pp. 963-986, 2008.
- [3] E. Kus, R. Grüninger, and R. Hüppi, "Integration of intelligent sensors for sensor guided motions in industrial robot applications," in *Proc. IEEE International Conference*, 2008.
- [4] F. Williams, E. Laithwaite, and L. Piggot, "Brushless variable speed induction motor," *IEEE Proceedings*, no. 2097U, pp. 102-118, 1956.
- [5] R. L. Hollis, A. P. Allan, and S. Salcudean, "A six-degree-of-freedom magnetically levitated variable compliance fine-motion wrist: Design, modeling, and control," *IEEE Transactions on Robotics and Automation*, 1991.
- [6] G. J. Vachtsevanos, K. Davey, and K. Lee, "Development of a novel intelligent robotic manipulator," *IEEE Control Systems Magazine*, vol. 7, no. 3, pp. 9-15, 1987.
- [7] K. Lee and C. Kwan, "Design concept development of a spherical stepper for robotic applications," *IEEE Transactions on Robotics and Automation*, vol. 7, no. 1, pp. 175-181, 1991.
- [8] J. B. Wang and D. G. Howe, "Analysis, design and control of a novel spherical permanent-magnet actuator," *IEEE Proceedings-Electric Power Applications*, vol. 145, no. 1, pp. 61-71, 1991.
- [9] K. Kahlen and R. Doncker, "Current regulators for multi-phase permanent magnet spherical machines," in *Proc. IEEE Industry Applications Conference*, vol. 3, pp. 2011-2016, 2000.
- [10] K. Kahlen, I. Voss, C. Priebe, and R. W. D. Doncker, "Torque control of a spherical machine with variable pole pitch," *IEEE Transactions on Power Electronics*, vol. 19, no. 6, pp. 1628-1634, 2004.
- [11] C. K. Lim, L. Yan, C. I. Ming, G. Yang, and W. Lin, "A novel approach in generating 3-DOF motions," in *Proc. IEEE International Conference on Mechatronics & Automation*, 2005.
- [12] M. Weyrich and M. W. Abdullah, "Concept of a three D.O.F spherical-joint gripper for industrial robots," in *Proc. IEEE 18th Conference on Emerging Technologies & Factory Automation*, 2013.
- [13] J. D. Robinson, J. B. Holland, M. J. D. Hayes, and R. G. Langlois, "Velocity-Level kinematics of the atlas spherical orienting device using omni-wheels," Dept. of Mechanical and Aerospace Engineering, Carleton University, 2005.
- [14] M. Hayes and R. Langlois, "Atlas: A novel kinematic architecture for six DOF motion platforms," *Transactions of the Canadian Society for Mechanical Engineering*, vol. 29, pp. 701-709, 2005.
- [15] M. Swartz, M. Hayes, and R. Langlois, "A complete kinematic and dynamic model for spherical actuation of the atlas motion platform," Department of Mechanical & Aerospace Engineering, Carleton University, Canada, 2006.
- [16] T. B. Lauwers, G. A. Kantor, and R. L. Hollis, "A dynamically stable single-wheeled mobile robot with inverse mouse-ball drive," in *Proc. IEEE International Conference on Robotics and Automation*, USA, May 2006.
- [17] J. Fong and S. Uppill, "899: Design and build a ballbot," Mech Eng 4135: Mechatronics Honours Project, The University of Adelaide, 2009.
- [18] C. W. Wu and C. K. Hwang, "A novel spherical wheel driven by omni-wheels," in *Proc. Seventh International Conference on Machine Learning and Cybernetics*, 2008, pp. 3800-3803.
- [19] M. Kumagai and T. Ochiai, "Development of a robot balanced on a ball," in *Proc. IEEE International Conference on Robotics and Automation Kobe*, Japan, May 2009.
- [20] A. Weiss, M. J. D. Hayes, and R. G. Langlois, "Atlas motion platform generalized kinematic model," *Meccanica*, vol. 46, no. 1, pp. 17-25, 2011.